

THE 4TH INTERNATIONAL CONFERENCE ON ALUMINUM ALLOYS

HOT COMPRESSION BEHAVIOR OF WROUGHT AL 6061*

Dan Zhao and Prabir K. Chaudhury
Concurrent Technologies Corporation
1450 Scalp Avenue, Johnstown, PA 15904, USA

Abstract

The flow behavior of Al 6061 was studied by conducting hot compression tests at various processing conditions used in the metalforming industry. The temperature and the strain rate ranges were 200 to 500 C and 0.001 to 20 s⁻¹ respectively. True stress-true strain flow curves were generated, and microstructural changes during elevated temperature deformation were characterized. Elongated grains were observed in specimens tested at low temperatures, dynamic recovery occurred at low and intermediate temperatures, and dynamic recrystallization occurred at high temperatures. The material exhibited complete recrystallization only at 500 C and 20 s⁻¹. The selection of hot working parameters for optimum processing is discussed on the basis of flow behavior and resulting microstructures.

Introduction

Al 6061 is an important wrought aluminum alloy commonly used in heavy-duty structures, such as trucks, marine applications, railroad cars, and pipelines, which require strength, corrosion resistance and weldability. Hot forming of Al 6061, a precipitation hardening alloy, involves thermally activated processes. To hot work this material efficiently, a thorough understanding of mechanical and microstructural behavior during high temperature deformation is essential. These material characteristics not only help design the hot forming processes, but provide guidelines for subsequent heat treatments.

In this investigation, the flow behavior of wrought Al 6061 was studied by conducting compression tests at various temperatures (200-500 C) and strain rates (0.001-20 s⁻¹). Microstructural changes during elevated temperature deformation were also characterized to help engineers select processing conditions for desired microstructures. The selection of processing conditions is discussed based on the analysis of flow behavior and the observation of microstructural changes.

Material and Experimental Procedure

Commercially available 19 mm diameter extruded Al 6061-T651 bar was used in this investigation. Table I lists the chemical composition of the alloy, and Figure 1 shows the typical microstructure of the as-received material. The as-received microstructure consisted of large elongated grains, as long as 1.25 mm. Fine precipitates, most likely Mg₂Si, were present along grain boundaries.

This work was conducted by the National Center for Excellence in Metalworking Technology, operated by Concurrent Technologies Corporation, under contract to the U.S. Navy as part of the U.S. Navy Manufacturing Technology Program.

Table I. Chemical Composition of Al 6061 (wt. %)

Mg	Si	Cu	Fe	Cr	Zn	Ti	Mn	Al
1.00	0.60	0.275	0.70	0.195	0.25	0.15	0.15	Bal.

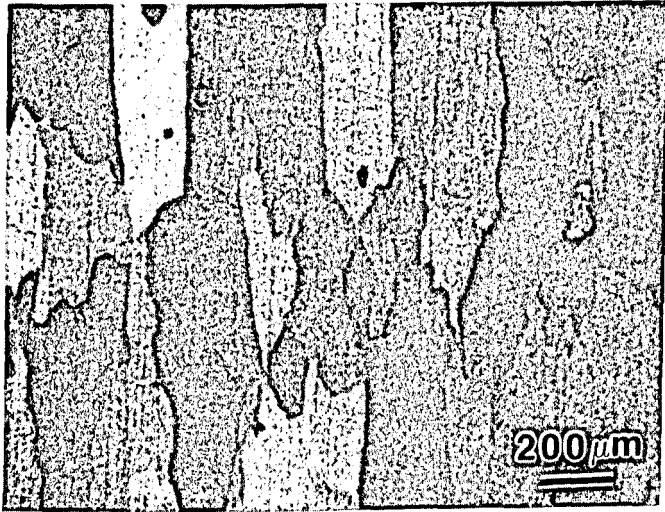


Figure 1. As-received microstructure of Al 6061.

Cylindrical compression test specimens with a diameter of 12.7 mm and a height of 15.9 mm were machined from the bar. Isothermal compression tests were conducted on a servo-hydraulic MTS machine. Boron nitride was used as the lubricant between the specimen and the TBM platens. The testing was conducted at temperatures 200, 250, 300, 350, 400, 450, and 500 C and strain rates 0.001, 0.01, 0.03, 0.1, 0.3, 1, 5 and 20 s⁻¹.

Prior to compression, specimens were soaked for 10 minutes at the test temperature. Load and stroke were acquired during the compression test by a data acquisition system and later converted to true stress-true strain curves. Immediately after the compression test, the specimens were quenched in to retain the deformed microstructure. Longitudinal sections were examined by optical microscopy. Grain size was measured by the linear intercept method, and Vickers hardness was measured using a load of 100 g and a dwell time of 10 seconds.

Results and Discussion

Flow Behavior and As-deformed Microstructure

The flow curves and as-deformed microstructures were reported elsewhere [1]. Three types of flow curves after initial hardening were apparent: (a) steady state flow; (b) flow softening; and (c) flow hardening. These three types of flow curves are schematically illustrated in Figure 2. During initial stages of deformation, the hardening rate is very high, and decreases with strain as dislocation generation or multiplication process slows down due to the increased dislocation density that approaches saturation. In contrast, the predominant softening processes such as dynamic recovery (DRV) are thermally activated, and both temperature and time play important

roles in balancing the hardening rate leading to a steady state. The three types of flow curves are manifestation of this time-temperature effect on microstructural changes during the hot deformation process.

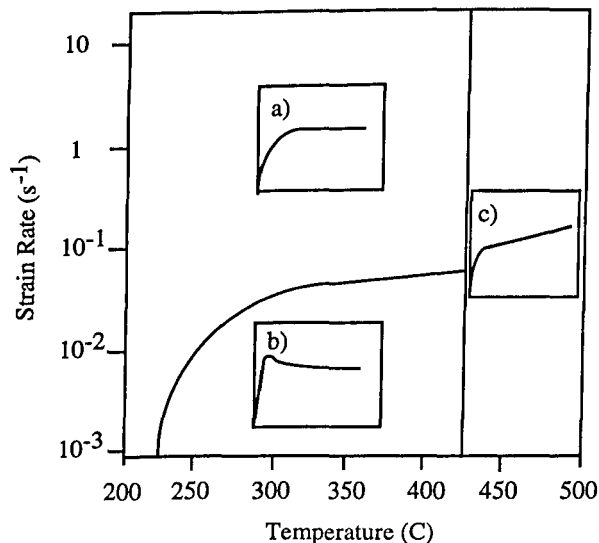


Figure 2. A schematic of the three types of flow curves as function of temperature and strain rate.

Steady state flow, the first type of flow curve, occurred at all strain rates for the lowest test temperature (200 C), as well as at intermediate to high strain rates in the intermediate temperature range (250-400 C). Under these conditions, initially the hardening rate is higher than the softening rate, but with time or strain, the softening rate becomes comparable to the hardening rate and steady state flow is approached. The low temperature and/or limited time available (at high strain rates) were not sufficient to supersede the hardening rate. The steady state flow resulted from the balance of the hardening and softening (recovery) processes in the alloy.

As the temperature increased (≥ 250 C), thermally activated restoration processes such as dynamic recovery (DRV) became dominant at low strain rates after initial hardening before reaching the steady state. Inhomogeneous flow, especially at high strains, also contributed to the softening, as shown in Figure 3. In addition, over-aging at these temperatures and strain rates may have contributed to softening. Under these conditions, the DRV process, through formation of dislocation networks, subgrains and cellular structure, exhibited a high rate of softening and resulted in a drop in the flow stress following the peak stress. After the initial impact of DRV, the flow reached a steady state where rates of hardening and softening became equal, resulting in the second type of flow curve. At higher strain rates, however, the flow curves were of the first type because the time at test temperature was much less, and softening could only balance the high rate of hardening.

The third type of flow curve was observed at high temperatures (450-500 C). In this case, continued flow hardening was observed. The as-deformed specimens were partially or fully recrystallized, Figures 4 and 5. At these high temperatures, dynamic recrystallization took place early and continued hardening was observed, possibly due to strain hardening of the newly recrystallized grains. The extent of hardening increased with increasing temperature and/or

decreasing strain rate, the conditions at which dynamic recrystallization is enhanced. Under some conditions, wavy flow curves (Figure 6), showing continuous dynamic recrystallization and overall strain hardening were observed. In addition, the softening contribution from inhomogeneous flow was limited at these temperatures. Figure 7 shows that the deformation is more uniform compared to that at lower temperatures, Figure 3.

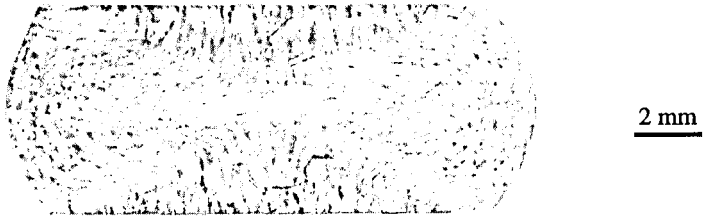


Figure 3. Inhomogeneous flow in some specimens deformed to a true strain of 0.8, 350 C and 0.001 s^{-1} in this case.

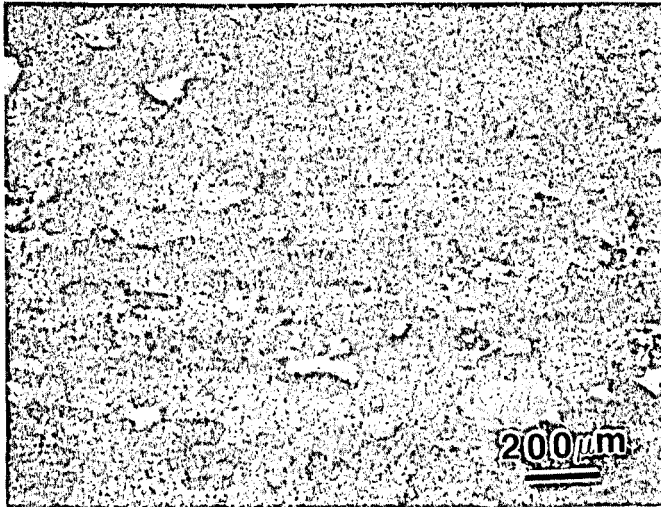


Figure 4. Photomicrograph showing as-deformed microstructure (true strain of 0.8) with partial recrystallization, 450 C and 20 s^{-1} .

The hardness values on the quenched specimens after hot deformation were plotted in Figure 8 for three temperatures as a function of strain rate. Results indicate that the room temperature hardness of the material is strongly influenced by the precipitation behavior of the alloy. The as-received (T651 condition) hardness of 120 VPN is typical of peak aged and cold finished Al 6061, while deformation at 200 C showed continued decrease in hardness due to DRV as deformation time increased (strain rate decreased). The lowest hardness (50 VPN) observed for specimens deformed at 350 C indicates extensive overaging of the microstructure, similar to the fully annealed condition. However, the increased hardness of specimens deformed at 500 C indicates solid solution strengthening of the alloy as some of the precipitates go into solution at this temperature and natural aging of the microstructure occurs, similar to the T4 condition. The room temperature

hardness values of the deformed specimens not only confirmed that microstructural changes occurred during hot deformation, which also helps minimize or modify subsequent heat treatment for requisite service properties.

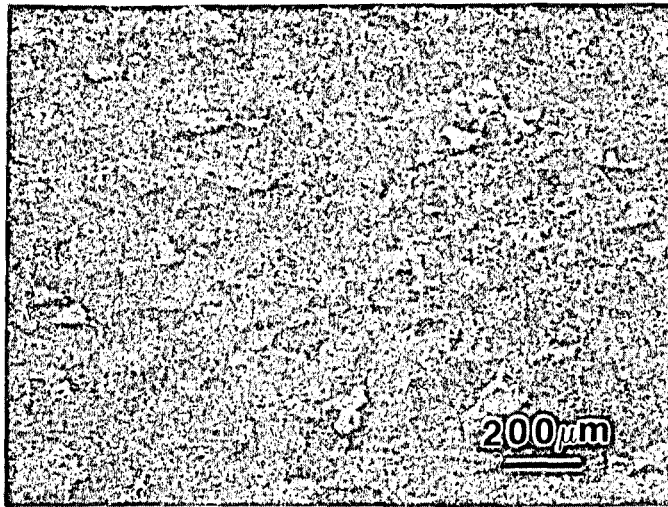


Figure 5. Photomicrograph showing as-deformed microstructure (true strain of 0.8) with complete recrystallization, 500 C and 20 s⁻¹.

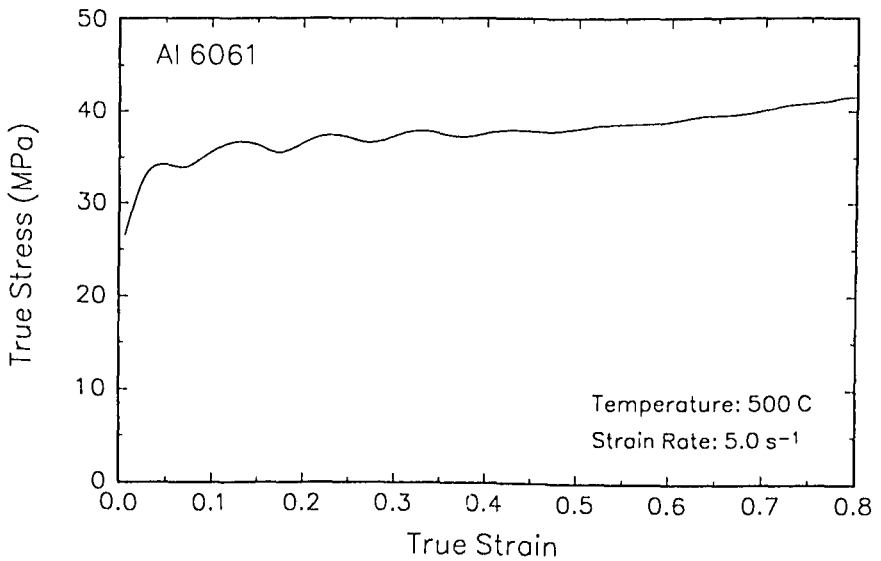


Figure 6. Flow curve showing repeated hardening and softening at 500 C and 5 s⁻¹.

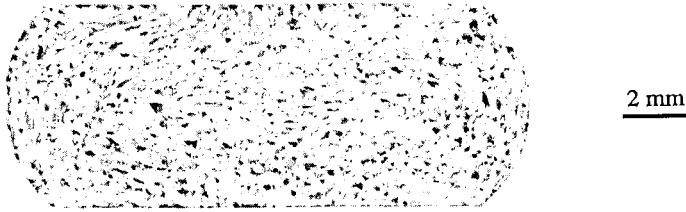


Figure 7. Example of relatively uniform flow, true strain of 0.8, 500 C and 0.001 s^{-1} .

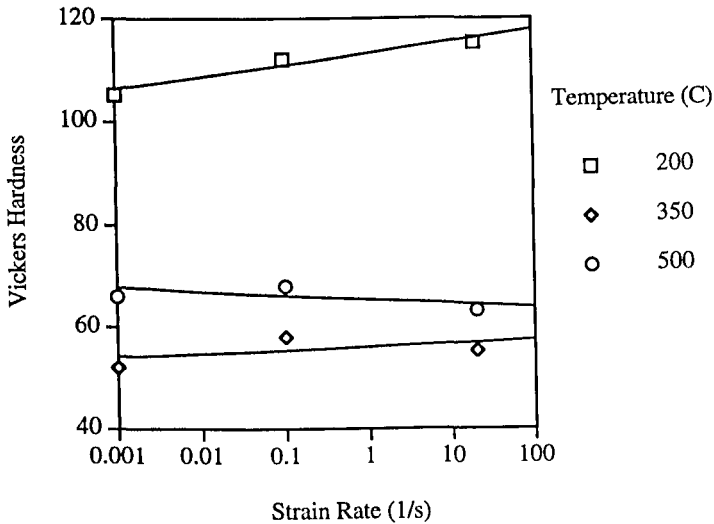


Figure 8. Room temperature hardness values on the specimens deformed at various temperatures and strain rates.

Flow stress values at a true strain of 0.5 were plotted as a function of strain rate on a log-log scale for each temperature in Figure 9. The plots, except the one at 200 C, show a transition at strain rates ranging from 10^{-2} to 1 s^{-1} , depending on the temperature. This transition, where the slope or the strain rate sensitivity changed from 0.21 (dislocation climb controlled) to a lower value, is consistent with power law breakdown observed in Al alloys [2-4]. With decreasing temperature, the transition strain rate decreases, and at the lowest temperature (200 C) the strain rate sensitivity is very low (~ 0.03) over the entire range of strain rate tested. This behavior is also typical of solid solutions [4, 5] which exhibit exponential stress dependence and smaller activation energy than that for lattice self diffusion at low temperatures and very high strain rates. Figure 10 shows the effect of temperature on flow stress at the same true strain. The slopes of these plots are related to the apparent activation energy of deformation and the deformation substructure. The large variation in substructure at higher temperatures results in a wider variation in the slope. It is also apparent that the rate controlling flow mechanism changes with decreasing temperature to 200 C, where the activation energy is lower due to increased contribution from other mechanisms, such as dislocation pipe diffusion [5].

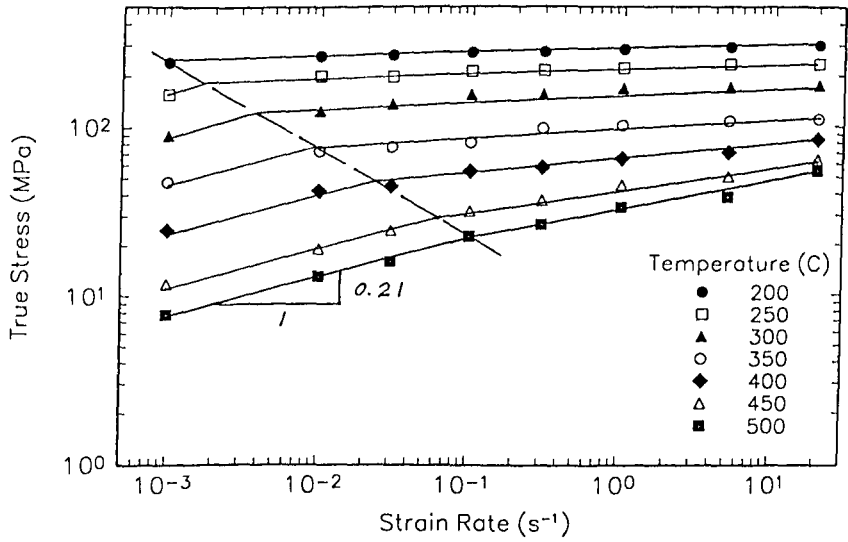


Figure 9. Effect of strain rate on flow stress for Al 6061 at a true strain of 0.5.

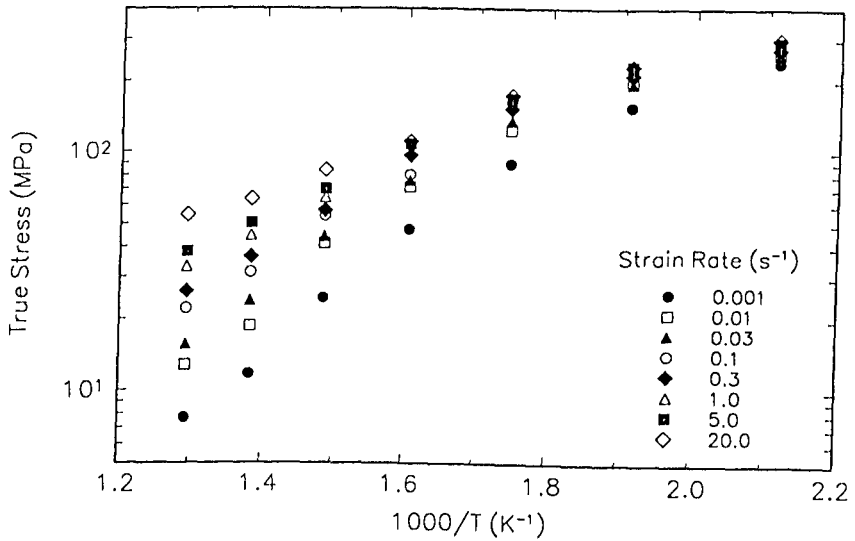


Figure 10. Effect of temperature on flow stress for Al 6061 at a true strain of 0.5.

Summary

High temperature deformation of Al 6061 was studied by conducting compression tests over a wide range of temperatures and strain rates. Three types of flow curves were observed: (a) steady state flow at the lowest temperature (200 C) and all strain rates, as well as at intermediate temperatures (250-400 C) and intermediate to high strain rates ($\geq 0.1 \text{ s}^{-1}$); (b) flow softening at intermediate temperatures (250-400 C) and low strain rates ($< 0.1 \text{ s}^{-1}$); and (c) flow hardening at high temperatures (450-500 C). Dynamic restoration processes were apparent at intermediate and high temperatures ($\geq 250 \text{ C}$). Partial recrystallization was observed at 450 to 500 C, except at 500 C and 20 s^{-1} , where the recrystallization was complete. Although the high temperature flow behavior reflects microstructural changes occurring during deformation, the specifics of deformed microstructure and flow inhomogeneity play important roles in deformation processing. Therefore, the optimum processing parameters must be tailored by considering flow behavior, post-deformation microstructure, and mechanical properties.

References

1. Atlas of Formability Bulletins - Aluminum 6061, Wrought (Johnstown, Pennsylvania, USA: National Center for Excellence in Metalworking Technology, 1994).
2. P. K. Chaudhury and F. A. Mohamed, Mat. Sci. Eng. A, 101 (1988), 13.
3. J. Weertman, Rate Processes in Plastic Deformation of Materials, ed J. C. M. Li and A. K. Mukherjee (Metals Park, Ohio, USA: ASM, 1975), 315.
4. S. C. Misro and A. K. Mukherjee, *ibid*, 434.
5. O. D. Sherby and C. M. Young, *ibid*, 497.